

Quantal Density Functional Theory of the Hydrogen Molecule

Xiao-Yin Pan and Viraht Sahni¹

¹*Department of Physics, Brooklyn College and The Graduate School of the City University of New York,
365 Fifth Avenue, New York, New York 10016.*

In this paper we perform a Quantal Density Functional Theory (Q-DFT) study of the Hydrogen molecule in its ground state. In common with traditional Kohn-Sham density functional theory (KS-DFT), Q-DFT transforms the interacting system as described by Schrodinger theory, to one of noninteracting fermions – the S system – such that the equivalent density, total energy, and ionization potential are obtained. The Q-DFT description of the S system is in terms of ‘classical’ fields and their quantal sources that are quantum-mechanical expectations of Hermitian operators taken with respect to the interacting and S system wave functions.. The sources, and hence the fields, are separately representative of all the many-body effects the S system must account for, viz. electron correlations due to the Pauli exclusion principle, Coulomb repulsion and Correlation-Kinetic effects. The local electron-interaction potential energy of each model fermion is the work done to move it in the force of a conservative effective field that is the sum of the individual fields. The Hartree, Pauli, Coulomb, and Correlation-Kinetic energy components of the total energy are also expressed in virial form in terms of the corresponding fields. The highest occupied eigenvalue of the S system is the negative of the ionization potential energy. The Q-DFT analysis of the Hydrogen molecule is performed employing the highly accurate correlated wave function of Kolos and Roothaan. The structure of the sources – the density, Fermi-Coulomb, Fermi, and Coulomb holes – as a function of the electron position are obtained, and from them the corresponding fields. (To our knowledge, these are the first accurate graphs of the Fermi-Coulomb and Coulomb holes as a function of electron position for the Hydrogen molecule.) As a consequence of the symmetry of the molecule, the individual fields – Hartree, Pauli, Coulomb, Correlation-Kinetic – are all *antisymmetric* about the center of the nuclear bond. Thus, the electron-interaction potential energy, and its Hartree, Pauli, Coulomb, and Correlation-Kinetic components are each *symmetric* about this center. The Coulomb correlation and Correlation-Kinetic fields, and hence their contributions to the potential and total energy are an order of magnitude smaller than those due to the Hartree and Pauli terms. However, the Correlation-Kinetic contribution is more significant than that due to Coulomb correlations. This new fact is important to the construction of approximate KS-DFT ‘correlation’ energy functionals for molecules. Finally, there is a striking similarity in the structure of the various sources, fields, and potential energies of the Hydrogen molecule for electron positions in the positive half-space encompassing one nucleus, and those of the

Helium atom.

I. INTRODUCTION

In this paper we analyze the Hydrogen molecule (H_2) in its ground-state electronic configuration $(\sigma_g 1s)^2$ from the perspective of time-independent Quantal density functional theory (Q-DFT) [1, 2, 3, 4, 5, 6, 7, 8]. The *in principle exact* framework of Q-DFT for ground and excited states, both nondegenerate and degenerate, has been demonstrated by application to exactly solvable model atomic systems [3, 5, 6, 7, 8] as well as by the use of essentially exact atomic correlated wave functions [2, 4, 9]. In its approximate form, Q-DFT has been applied to atoms, atomic ions, atoms in excited states, and positron binding, as well as to the many-electron inhomogeneity at metallic surfaces and metallic clusters. We refer the reader to the review articles of Refs [2, 10] for further references on these applications. This paper constitutes a first step in the application of Q-DFT to molecules. Here we present the essentially exact analysis of the H_2 molecule via Q-DFT by employing the highly accurate correlated wave function of Kolos and Roothaan [11]. Beyond the understandings achieved, a principal attribute of the calculation is the knowledge that the structure of the corresponding Q-DFT properties for other diatomic molecules will then be qualitatively similar. Furthermore, these essentially exact properties can be used as the basis for comparison and testing of various approximations within Q-DFT prior to their application to more complex molecules.

Q-DFT, in common with traditional Kohn-Sham density functional theory (KS-DFT)[12], maps a system of electrons in an external field $\mathbf{F}^{ext} = -\nabla v(\mathbf{r})$ in their *ground* state to one of *noninteracting* fermions in their *ground* state with equivalent density. The equivalent ground-state energy and ionization potential are thereby also obtained. The model system of noninteracting fermions is referred to as the S system, S being a mnemonic for a single Slater determinant. (Within the framework of Q-DFT, it is also possible *in principle* to map into an S system in which the noninteracting fermions are in an *excited* state.) The local (multiplicative) effective potential energy $v_s(\mathbf{r})$ of the model fermions is the sum of the external $v(\mathbf{r})$ and an electron-interaction $v_{ee}(\mathbf{r})$ potential energy, the latter being representative of all the electron correlations the S system must account for. These correlations are those due to the Pauli exclusion principle, Coulomb repulsion, and Correlation-Kinetic effects. The Correlation-Kinetic contribution is a consequence of the difference in the kinetic energies of the interacting and noninteracting systems with equivalent density. In Q-DFT, the potential energy $v_{ee}(\mathbf{r})$ is defined as the work done to move a model fermion in the force of a conservative ‘classical’ field. The components

of this field each separately represent a different electron correlation. The sources of these component fields are quantal in that they are expectations of Hermitian operators taken with respect to the Schrödinger and S system wave functions. The Pauli (exchange), Coulomb (correlation), and Correlation-Kinetic components of the total energy are also separately expressed in integral virial form in terms of the fields representative of these correlations. The highest occupied eigenvalue of the S system differential equation is the negative of the ionization potential[13].

The traditional KS-DFT description of the S system differs from that of Q-DFT in the following manner. Traditional theory is in terms of the ground state energy functional $E[\rho]$ of the density $\rho(\mathbf{r})$, and of its functional derivative. In KS-DFT, the many-body correlations noted above are embedded in the KS electron-interaction energy functional $E_{ee}^{KS}[\rho]$. The corresponding electron-interaction potential energy of the noninteracting fermions is defined as the functional derivative of this functional taken at the true ground state density value: $v_{ee}(\mathbf{r}) = \delta E_{ee}^{KS}[\rho]/\delta\rho(\mathbf{r})$. Within KS-DFT, it is common practice to subtract the known Hartree or Coulomb self energy functional $E_H[\rho]$ from $E_{ee}[\rho]$, thereby defining the KS ‘exchange-correlation’ energy functional $E_{xc}^{KS}[\rho]$ and its functional derivative $v_{xc}(\mathbf{r}) = \delta E_{xc}^{KS}[\rho]/\delta\rho(\mathbf{r})$. The functionals $(E_{ee}^{KS}[\rho], E_{xc}^{KS}[\rho])$ and their respective derivatives $(v_{ee}(\mathbf{r}), v_{xc}(\mathbf{r}))$ are therefore also representative of the Pauli and Coulomb correlations and Correlation-Kinetic effects. KS-DFT, however does not describe how the different electron correlations are incorporated in the functionals $(E_{ee}^{KS}[\rho], E_{xc}^{KS}[\rho])$ and hence how they are represented in their functional derivatives. Furthermore, the functionals $(E_{ee}^{KS}[\rho], E_{xc}^{KS}[\rho])$ are themselves unknown. As such, even if the exact wave function of an interacting system were known, it is not possible to construct the corresponding S system directly by following the prescription of KS-DFT. Hence, the potential energy $v_{xc}(\mathbf{r})$ is usually constructed indirectly via density-based methods [14-17] that employ knowledge of the ‘exact’ density as determined from *ab initio* calculations.

In Section II we give a brief description of ground state Q-DFT. Section III is a description of the various quantal sources, fields, energies and potential energies pertaining to the S system as determined via Q-DFT employing the 51-parameter correlated wave function of Kolos-Roothaan. Concluding remarks are made in Section IV.

II. Q-DFT OF A NONDEGENERATE GROUND STATE

The Schrödinger equation for a system of N electrons in an external field $\mathbf{F}^{ext}(\mathbf{r}) = -\nabla v(\mathbf{r})$, and in a nondegenerate ground state, is

$$[\hat{T} + \hat{V} + \hat{U}]\Psi(\mathbf{X}) = E\Psi(\mathbf{X}), \quad (1)$$

where $\hat{T} = -\frac{1}{2} \sum_i \nabla_i^2$, $\hat{V} = \sum_i v(\mathbf{r}_i)$, and $\hat{U} = \frac{1}{2} \sum_{i,j}' \frac{1}{|\mathbf{r}_i - \mathbf{r}_j|}$ are the kinetic energy, local external potential energy, and electron-interaction potential energy operators, $\Psi(\mathbf{X})$ and E are the ground state wave function and energy, with $\mathbf{X} = \mathbf{x}_1, \mathbf{x}_2, \dots, \mathbf{x}_N$, $\mathbf{x} = \mathbf{r}\sigma$, and \mathbf{r} and σ the spatial and spin coordinates. The ground state electronic density is the expectation

$$\rho(\mathbf{r}) = \langle \Psi | \hat{\rho} | \Psi \rangle, \quad (2)$$

where $\hat{\rho} = \sum_i \delta(\mathbf{r} - \mathbf{r}_i)$ is the Hermitian density operator. The corresponding spinless single particle density matrix is the expectation

$$\gamma(\mathbf{r}\mathbf{r}') = \langle \Psi | \hat{\gamma} | \Psi \rangle, \quad (3)$$

where the Hermitian operator $\hat{\gamma} = \hat{A} + i\hat{B}$, $\hat{A} = \frac{1}{2} \sum_j [\delta(\mathbf{r}_j - \mathbf{r})T_j(\mathbf{a}) + \delta(\mathbf{r}_j - \mathbf{r}')T_j(-\mathbf{a})]$, $\hat{B} = -\frac{i}{2} \sum_j [\delta(\mathbf{r}_j - \mathbf{r})T_j(\mathbf{a}) - \delta(\mathbf{r}_j - \mathbf{r}')T_j(-\mathbf{a})]$, $T_j(\mathbf{a})$ is a translation operator, and $\mathbf{a} = \mathbf{r}' - \mathbf{r}$. The diagonal matrix element of $\gamma(\mathbf{r}\mathbf{r}')$ is the density: $\gamma(\mathbf{r}\mathbf{r}) = \rho(\mathbf{r})$. The ground state energy is the expectation

$$E = \langle \Psi | \hat{T} + \hat{V} + \hat{U} | \Psi \rangle = T + E_{ext} + E_{ee}, \quad (4)$$

with the kinetic energy $T = \langle \Psi | \hat{T} | \Psi \rangle$, the external potential energy $E_{ext} = \langle \Psi | \hat{V} | \Psi \rangle = \int \rho(\mathbf{r})v(\mathbf{r})d\mathbf{r}$, and the electron-interaction energy $E_{ee} = \langle \Psi | \hat{U} | \Psi \rangle$. The ionization potential is $I = E^{ion} - E$, where E^{ion} is the energy of the resulting ion when the least bound electron is removed to infinity.

The differential equation for the S-system in its ground state that leads to the same density $\rho(\mathbf{r})$ as that of the electrons is

$$[-\frac{1}{2}\nabla^2 + v(\mathbf{r}) + v_{ee}(\mathbf{r})]\phi_i(\mathbf{x}) = \epsilon_i\phi_i(\mathbf{x}); \quad i = 1, \dots, N, \quad (5)$$

where $v_{ee}(\mathbf{r})$ is the electron-interaction potential energy of the noninteracting fermions. The S system wave function is the Slater determinant $\Phi\{\phi_i(\mathbf{x})\}$ of the orbitals $\phi_i(\mathbf{x})$, so that the density

is the expectation

$$\rho(\mathbf{r}) = \langle \Phi\{\phi_i\} | \hat{\rho} | \Phi\{\phi_i\} \rangle = \sum_i \sum_{\sigma} |\phi_i(\mathbf{r}\sigma)|^2, \quad (6)$$

and the corresponding spinless Dirac density matrix is the expectation

$$\gamma_s(\mathbf{r}\mathbf{r}') = \langle \Phi\{\phi_i\} | \hat{\gamma} | \Phi\{\phi_i\} \rangle = \sum_i \sum_{\sigma} \phi_i^*(\mathbf{r}\sigma) \phi_i(\mathbf{r}'\sigma). \quad (7)$$

The potential energy $v_{ee}(\mathbf{r})$ is the work done to move the model fermion from a reference point at infinity to its position at \mathbf{r} in the force of a *conservative* effective field $\mathcal{F}^{eff}(\mathbf{r})$:

$$v_{ee}(\mathbf{r}) = - \int_{\infty}^{\mathbf{r}} \mathcal{F}_k^{eff}(\mathbf{r}') \cdot d\mathbf{l}'. \quad (8)$$

The field $\mathcal{F}_k^{eff}(\mathbf{r})$ is the sum of an electron-interaction field $\mathcal{E}_{ee}(\mathbf{r})$ representative of Pauli and Coulomb correlations, and a Correlation-Kinetic field $\mathcal{Z}_{tc}(\mathbf{r})$ that is representative of the correlation contribution to the kinetic energy:

$$\mathcal{F}^{eff}(\mathbf{r}) = \mathcal{E}_{ee}(\mathbf{r}) + \mathcal{Z}_{tc}(\mathbf{r}). \quad (9)$$

The field $\mathcal{E}_{ee}(\mathbf{r})$ is obtained via Coulomb's law from its quantal source $g(\mathbf{r}\mathbf{r}')$, the pair-correlation density. Thus,

$$\mathcal{E}_{ee}(\mathbf{r}) = \int \frac{g(\mathbf{r}\mathbf{r}')(\mathbf{r} - \mathbf{r}')}{|\mathbf{r} - \mathbf{r}'|^3} d\mathbf{r}', \quad (10)$$

where $g(\mathbf{r}\mathbf{r}') = \langle \Psi | \hat{P}(\mathbf{r}\mathbf{r}') | \Psi \rangle / \rho(\mathbf{r})$, and $\hat{P}(\mathbf{r}\mathbf{r}') = \sum_{i,j}' \delta(\mathbf{r}_i - \mathbf{r}) \delta(\mathbf{r}_j - \mathbf{r}')$ the Hermitian pair-correlation operator. The pair-correlation density may be further separated into its local(static) and nonlocal (dynamic) components as

$$g(\mathbf{r}\mathbf{r}') = \rho(\mathbf{r}') + \rho_{xc}(\mathbf{r}\mathbf{r}') \quad (11)$$

$$= \rho(\mathbf{r}') + \rho_x(\mathbf{r}\mathbf{r}') + \rho_c(\mathbf{r}\mathbf{r}'), \quad (12)$$

where the sources $\rho_{xc}(\mathbf{r}\mathbf{r}')$, $\rho_x(\mathbf{r}\mathbf{r}')$, and $\rho_c(\mathbf{r}\mathbf{r}')$ are the Fermi-Coulomb, Fermi, and Coulomb hole charge distributions. The Fermi hole is defined as $\rho_x(\mathbf{r}\mathbf{r}') = -|\gamma_s(\mathbf{r}\mathbf{r}')|^2 / 2\rho(\mathbf{r})$, and the Coulomb hole is defined via Eqs.(11) and (12). The sum rules satisfied by these charge distributions are $\int \rho_{xc}(\mathbf{r}\mathbf{r}') d\mathbf{r}' = -1$; $\int \rho_x(\mathbf{r}\mathbf{r}') d\mathbf{r}' = -1$; $\rho_x(\mathbf{r}\mathbf{r}') \leq 0$; $\rho_x(\mathbf{r}\mathbf{r}) = -\rho(\mathbf{r})/2$, and $\int \rho_c(\mathbf{r}\mathbf{r}') d\mathbf{r}' = 0$. With

the above separation, the electron-interaction field may then be written in terms of its components as

$$\mathcal{E}_{ee}(\mathbf{r}) = \mathcal{E}_H(\mathbf{r}) + \mathcal{E}_{xc}(\mathbf{r}) \quad (13)$$

$$= \mathcal{E}_H(\mathbf{r}) + \mathcal{E}_x(\mathbf{r}) + \mathcal{E}_c(\mathbf{r}), \quad (14)$$

where the Hartree $\mathcal{E}_H(\mathbf{r})$, Pauli-Coulomb $\mathcal{E}_{xc}(\mathbf{r})$, Pauli $\mathcal{E}_x(\mathbf{r})$, and Coulomb $\mathcal{E}_c(\mathbf{r})$ fields are due to their respective quantal sources $\rho(\mathbf{r})$, $\rho_{xc}(\mathbf{r}\mathbf{r}')$, $\rho_x(\mathbf{r}\mathbf{r}')$, and $\rho_c(\mathbf{r}\mathbf{r}')$.

The Correlation-Kinetic field $\mathcal{Z}_{tc}(\mathbf{r})$ is the difference of the kinetic fields $\mathcal{Z}(\mathbf{r})$ and $\mathcal{Z}_s(\mathbf{r})$ of the interacting and noninteracting systems, respectively:

$$\mathcal{Z}_{tc}(\mathbf{r}) = \mathcal{Z}_s(\mathbf{r}) - \mathcal{Z}(\mathbf{r}), \quad (15)$$

where $\mathcal{Z}(\mathbf{r}) = \mathbf{z}(\mathbf{r}; [\gamma])/\rho(\mathbf{r})$ and $\mathcal{Z}_s(\mathbf{r}) = \mathbf{z}_s(\mathbf{r}; [\gamma_s])/\rho(\mathbf{r})$. The quantal sources of the fields $\mathcal{Z}(\mathbf{r})$ and $\mathcal{Z}_s(\mathbf{r})$ are the single particle and Dirac density matrices. The kinetic ‘force’ $\mathbf{z}(\mathbf{r}; [\gamma])$ is defined in terms of its components as $z_\alpha(\mathbf{r}; [\gamma]) = 2 \sum_\beta \partial t_{\alpha\beta}(\mathbf{r}; [\gamma]) / \partial r_\beta$, where $t_{\alpha\beta}(\mathbf{r}; [\gamma]) = \frac{1}{4} [\partial^2 / \partial r'_\alpha \partial r''_\beta + \partial^2 / \partial r'_\beta \partial r''_\alpha] \gamma(\mathbf{r}'\mathbf{r}'')|_{\mathbf{r}'=\mathbf{r}''=\mathbf{r}}$ is the kinetic energy tensor. The field $\mathbf{z}_s(\mathbf{r}; [\gamma_s])$ is similarly defined in terms of the S-system tensor $t_{\alpha\beta,s}(\mathbf{r}; [\gamma_s])$.

The Hartree field $\mathcal{E}_H(\mathbf{r})$ is conservative, and $\nabla \times \mathcal{E}_H(\mathbf{r}) = 0$. This is because its source $\rho(\mathbf{r})$ is a static charge, and the field may consequently be written as $\mathcal{E}_H(\mathbf{r}) = -\nabla W_H(\mathbf{r})$, where $W_H(\mathbf{r}) = \int d\mathbf{r}' \rho(\mathbf{r}')/|\mathbf{r} - \mathbf{r}'|$. The fields $\mathcal{E}_{xc}(\mathbf{r})$, $\mathcal{E}_x(\mathbf{r})$, and $\mathcal{E}_c(\mathbf{r})$ are in general not conservative as their sources are nonlocal. The sum of the fields $\mathcal{E}_{xc}(\mathbf{r}) + \mathcal{Z}_{tc}(\mathbf{r})$ and $\mathcal{E}_x(\mathbf{r}) + \mathcal{E}_c(\mathbf{r}) + \mathcal{Z}_{tc}(\mathbf{r})$ are always conservative.

For systems of symmetry such that the component fields $\mathcal{E}_{ee}(\mathbf{r})$ and $\mathcal{Z}_{tc}(\mathbf{r})$ are separately conservative, the potential energy $v_{ee}(\mathbf{r})$ may be expressed as the sum of the separate work done in these fields. Thus

$$v_{ee}(\mathbf{r}) = W_{ee}(\mathbf{r}) + W_{tc}(\mathbf{r}) \quad (16)$$

$$= W_H(\mathbf{r}) + W_{xc}(\mathbf{r}) + W_{tc}(\mathbf{r}) \quad (17)$$

$$= W_H(\mathbf{r}) + W_x(\mathbf{r}) + W_c(\mathbf{r}) + W_{tc}(\mathbf{r}), \quad (18)$$

where $W_{ee}(\mathbf{r})$, $W_H(\mathbf{r})$, $W_{xc}(\mathbf{r})$, $W_x(\mathbf{r})$, $W_c(\mathbf{r})$, and $W_{tc}(\mathbf{r})$ are respectively the work done in the fields $\mathcal{E}_{ee}(\mathbf{r})$, $\mathcal{E}_H(\mathbf{r})$, $\mathcal{E}_{xc}(\mathbf{r})$, $\mathcal{E}_x(\mathbf{r})$, $\mathcal{E}_c(\mathbf{r})$, and $\mathcal{Z}_{tc}(\mathbf{r})$.

The ground state energy is

$$E = T_s + \int \rho(\mathbf{r})v(\mathbf{r})d\mathbf{r} + E_{ee} + T_c, \quad (19)$$

where $T_s = \langle \Phi\{\phi_i\}|\hat{T}|\Phi\{\phi_i\} \rangle$ is the kinetic energy of the noninteracting Fermions. The electron-interaction E_{ee} and Correlation-Kinetic T_c energies are expressed in terms of the fields $\mathcal{E}_{ee}(\mathbf{r})$ and $\mathcal{Z}_{t_c}(\mathbf{r})$, respectively, in integral virial form as

$$E_{ee} = \int d\mathbf{r}\rho(\mathbf{r})\mathbf{r} \cdot \mathcal{E}_{ee}(\mathbf{r}) \quad \text{and} \quad T_c = \frac{1}{2} \int d\mathbf{r}\rho(\mathbf{r})\mathbf{r} \cdot \mathcal{Z}_{t_c}(\mathbf{r}). \quad (20)$$

These expressions for the energy are valid whether the fields $\mathcal{E}_{ee}(\mathbf{r})$ and $\mathcal{Z}_{t_c}(\mathbf{r})$ are separately conservative or not. Employing Eq.(13) and (14) in Eq.(20), the energy E_{ee} may be written as a sum of the Hartree E_H and Pauli-Coulomb E_{xc} (or Pauli E_x plus Coulomb E_c) energies with each component term expressed in integral virial form.

Finally, the highest occupied eigenvalue of the S system differential equation is the negative of the ionization potential: $\epsilon_m = -I$.

III. APPLICATION TO THE HYDROGEN MOLECULE

A. Wave functions, Orbitals, and Density

The purely electronic part of the Hamiltonian for H_2 in atomic units ($e = m = \hbar = 1$) is

$$\hat{H} = -\frac{1}{2}\nabla_1^2 - \frac{1}{2}\nabla_2^2 - \frac{1}{r_{1a}} - \frac{1}{r_{2a}} - \frac{1}{r_{1b}} - \frac{1}{r_{2b}} + \frac{1}{r_{12}} \quad (21)$$

where 1 and 2 are the electrons, and a and b are the nuclei. As the wave function of the molecule in its ground state is unknown, we employ the essentially exact 51-parameter correlated wave function of Kolos-Roothaan [11] in our calculations. The symmetric spatial part of the wave function is

$$\Psi(\mathbf{r}_1\mathbf{r}_2) = \exp[-\delta(\xi_1 + \xi_2)] \sum_{mnjkl} C_{mnjkl} [\xi_1^m \xi_2^n \eta_1^j \eta_2^k + \xi_1^n \xi_2^m \eta_1^k \eta_2^j] r_{12}^p \quad (22)$$

with

$$\xi_1 = (r_{1a} + r_{1b})/R; \quad \xi_2 = (r_{2a} + r_{2b})/R; \quad (23)$$

$$\eta_1 = (r_{1a} - r_{1b})/R; \quad \eta_2 = (r_{2a} - r_{2b})/R, \quad (24)$$

where the variational parameters are δ and the coefficients C_{mnjkp} , $r_{12} = |\mathbf{r}_1 - \mathbf{r}_2|$, and $R = 2a$ is the internucleus separation. The values of the variational parameters are given in the Appendix. The total energy (inclusive of the internuclear potential energy $V_{nn} = 1/R$) is $E_{tot}(H_2) = -1.174448$ (a.u.) at $a = 0.7005$ (a.u.). The kinetic energy $T = -E_{tot}$, and the total potential energy $E_{ext} + E_{ee} + V_{nn} = -2.348851$ (a.u.). The virial theorem ratio, which is the ratio of the total potential energy to twice the total energy, is 0.999981. The electron interaction energy component $E_{ee} = 0.58737$ (a.u.), and the external energy $E_{ext} = -3.65005$ (a.u.). The total energy [18] of the Hydrogen molecular ion H_2^+ at the equilibrium internuclear separation of the Hydrogen molecule is $E_{tot}(H_2^+)|_{a=0.7005} = -0.56998$ (a.u.). Thus, the ionization potential of the H_2 molecule is $I = E_{tot}(H_2^+)|_{a=0.7005} - E_{tot}(H_2) = 0.60447$ (a.u.).

For two electron systems such as the Hooke's atom[19], Helium atom, or the Hydrogen molecule, the orbitals of the S system in its ground (singlet) state that lead to the interacting system density are known. These orbitals are $\phi_i(\mathbf{r}) = \sqrt{\rho(\mathbf{r})/2}$, $i = 1, 2$, and are therefore known to the same accuracy as the wave function or density.

The density $\rho(0, z)$ along the nuclear bond z-axis is plotted in Fig.1. The density is extremely accurate throughout space except at and very near each nucleus. Thus, although on the scale of this figure, it appears that the density satisfies the electron-nucleus cusp condition[20] exactly, in fact it does not.

B. Fermi-Coulomb, Fermi, and Coulomb Holes

For the H_2 molecule in its singlet ground state, there are no correlations due to the Pauli exclusion principle as the two electrons have opposite spin. However, within the S system framework, it is customary in local effective potential energy theories to define a Fermi hole as $\rho_x(\mathbf{r}\mathbf{r}') = -\rho(\mathbf{r}')/2$. (This is because the pair-correlation density as determined from the corresponding S system wave function is $g(\mathbf{r}\mathbf{r}') = \rho(\mathbf{r}')/2$.)

In Fig.2 we plot cross-sections through the Fermi-Coulomb $\rho_{xc}(\mathbf{r}\mathbf{r}')$, Fermi $\rho_x(\mathbf{r}\mathbf{r}')$, and Coulomb $\rho_c(\mathbf{r}\mathbf{r}')$ hole sources as a function of $\mathbf{r}' = (0, z')$ for an electron at the origin $\mathbf{r} = (0, 0)$ at the center of the nuclear bond. (Because of the cylindrical symmetry of the molecule, cylindrical coordinates are employed throughout.) The electron position is indicated by the arrow. The three

charge distributions, of course, have cylindrical symmetry about the bond axis. More significantly, they are symmetrical about the electron along the z' axis. Observe that at the electron position, both the Fermi-Coulomb and Coulomb holes exhibit a cusp corresponding to the electron-electron cusp condition [20]. (Based on the work of Ref. [21] it is known that the wave function does not satisfy this cusp condition exactly. It obviously satisfies it to a good degree as evidenced by the figure.) As expected, at the electron position, the Fermi-Coulomb hole is more negative than the Fermi hole. Thus, in the region about the electron, the Coulomb hole is negative. (This is also the case for all the other electron positions considered.) As both the Fermi-Coulomb and Fermi holes satisfy the same charge conservation sum rule, there must then be regions where the former lies above the latter. This is clearly evident in the figure. Hence, in the outer and classically forbidden regions of the molecule, the Coulomb hole is positive. (The positive part of the Coulomb hole is more clearly evident in the figures that follow.) The Coulomb hole is both positive and negative as its total charge is zero. The positive part of the Coulomb hole is an indication that the other electron is equally likely to be in the classically forbidden region on either side of each nucleus.

As the Fermi hole is independent of electron position, we now focus on the Fermi-Coulomb and Coulomb holes. In Figs.3-5, we plot the cross-sections of these holes for electron positions at $\mathbf{r} = (0, a/3)$, $\mathbf{r} = (0, 2a/3)$, $\mathbf{r} = (0, a)$. Again, observe the cusp at the electron position for both the Fermi-Coulomb and Coulomb holes of each figure. Note also how the positive part of the Coulomb hole becomes more pronounced relative to the negative part as the electron is moved away from the center of the nuclear bond towards one nucleus. The positive part of the Coulomb hole is also largest about the other nucleus, thereby indicating that the second electron is about this nucleus.

In Figs.6-8, we plot the Fermi-Coulomb and Coulomb hole cross-sections for an electron in the classically forbidden region at $\mathbf{r} = (0, 2a)$, $\mathbf{r} = (0, 4a)$, and $\mathbf{r} = (0, 6a)$. The positive part of the Coulomb hole continues to increase about the left nucleus at the expense of the negative part as the electron is moved further from the molecule. Thus, even for the asymptotic position of an electron at $\mathbf{r} = (0, 6a)$, the other electron is still mainly about the left nucleus. For all electron positions, the Fermi-Coulomb hole $\rho_{xc}(\mathbf{r}\mathbf{r}')$ is negative.

(We note that the same cross-sections of the Fermi-Coulomb, Fermi, and Coulomb holes for an electron position 0.3 (a.u.) to the left of the right nucleus, which corresponds approximately to our Fig.4, has been plotted by Baerends et al [22] in their study of the dissociation of the molecule.

However, in their figure, the electron-electron cusp in the Fermi-Coulomb and Coulomb holes is not present because the wave function employed by these authors is a configuration-interaction type wave function.)

C. Fields, Potential Energies, and Energies.

The electron-interaction field $\mathcal{E}_{ee}(\mathbf{r})$, and its Hartree $\mathcal{E}_H(\mathbf{r})$ and Pauli-Coulomb $\mathcal{E}_{xc}(\mathbf{r})$ components along the nuclear bond axis are plotted in Fig.9. Observe that these fields all vanish at the center of the bond axis or origin. This is because their corresponding sources – the pair-correlation density $g(\mathbf{r}\mathbf{r}')$, the density $\rho(\mathbf{r})$, and the Fermi-Coulomb hole charge $\rho_{xc}(\mathbf{r}\mathbf{r}')$ — are symmetrical about the center of the nuclear bond for this electron position (see Figs.1 and 2). The existence (non-zero value) of these fields for all other electron positions is a consequence of the fact that their sources are *not symmetrical* about the electron (see Figs.1 and 3-8). The fields are also all *antisymmetric* about the center of the nuclear bond. (This is a reflection of the symmetry about the x-y plane at the center of the nuclear bond. As such the potential energies obtained from these fields will be *symmetric* about this point.) In the positive half-space, there is a maximum in the electron-interaction and Hartree fields, and a minimum in the Pauli-Coulomb field. The Hartree and Pauli-Coulomb fields are of the same order of magnitude and opposite in sign. This is because their sources, $\rho(\mathbf{r})$ and $\rho_{xc}(\mathbf{r}\mathbf{r}')$ respectively, are of the same order of magnitude and opposite in sign. Asymptotically, in the z direction these fields decay as $\mathcal{E}_{ee}(\mathbf{r}) \sim 1/z^2$, $\mathcal{E}_H(\mathbf{r}) \sim 2/z^2$, and $\mathcal{E}_{xc}(\mathbf{r}) \sim -1/z^2$ as they must [3, 9]. (It is interesting to note that with a slight translation to the right, the plots of the fields in the positive half-space, are strikingly similar to those of the Helium atom [2, 9].)

The Pauli $\mathcal{E}_x(\mathbf{r})$ and Coulomb $\mathcal{E}_c(\mathbf{r})$ field components of the Pauli-Coulomb field $\mathcal{E}_{xc}(\mathbf{r})$ along the nuclear bond axis are plotted in Fig.10. Again, these fields vanish at the origin and are *antisymmetric* about it. Hence, the corresponding potential energies obtained from these fields will be symmetric. In the positive half space, the Pauli field $\mathcal{E}_x(\mathbf{r})$ is negative as its source is a negative charge. The Coulomb field $\mathcal{E}_c(\mathbf{r})$, on the other hand, is positive in the inter-nuclear region and negative throughout the region beyond the right nucleus. This structure is attributable to the fact that the Coulomb hole has both a positive and negative component. Asymptotically, the Pauli field decays as $\mathcal{E}_x(\mathbf{r}) \sim -1/z^2$, whereas the Coulomb field $\mathcal{E}_c(\mathbf{r})$ has essentially vanished by about $z = 5$ (a.u.). (Once again in the positive half-space, the structure of these fields when

translated slightly to the right, is similar to those of the Helium atom. In particular, we note that the structure of the Coulomb holes of the Hydrogen molecule for electron positions $z > a$ (see Figs. 6-8) is very similar to those of the Helium atom for electron positions away from its nucleus (see Figs.3,4 of [9]).) As is the case for atoms, it turns out that the asymptotic structure along the nuclear bond axis of $\{\mathcal{F}^{eff}(\mathbf{r}) - \mathcal{E}_H(\mathbf{r})\} \sim \mathcal{E}_x(\mathbf{r}) \sim -1/z^2$. Thus, the asymptotic structure of the electron-interaction potential energy $v_{ee}(\mathbf{r})$ minus the Hartree potential energy $W_H(\mathbf{r})$ is again due to Pauli correlations: $\{v_{ee}(\mathbf{r}) - W_H(\mathbf{r})\} \sim W_x(\mathbf{r}) \sim -1/z$ as shown in Fig. 11.

Since in the S system description of two electron systems $\mathcal{E}_x(\mathbf{r}) = -\mathcal{E}_H(\mathbf{r})/2$, the curl of the Fermi field along the nuclear bond z axis direction vanishes: $\nabla \times \mathcal{E}_x(\mathbf{r})|_z = 0$, as it does in all directions. Hence, the work done $W_x(0, z)$ plotted in Fig. 11 is path independent. Along the nuclear bond axis, however, the $\nabla \times \mathcal{E}_c(\mathbf{r})|_z \neq 0$ and $\nabla \times \mathcal{Z}_{t_c}(\mathbf{r})|_z \neq 0$. But in this and all directions, the curl of the sum of the fields $\mathcal{E}_c(\mathbf{r})$ and $\mathcal{Z}_{t_c}(\mathbf{r})$ vanishes: $\nabla \times [\mathcal{E}_c(\mathbf{r}) + \mathcal{Z}_{t_c}(\mathbf{r})]|_z = 0$. Therefore, the work done in the sum of these fields in all directions, and hence along the nuclear bond axis $v_c(0, z) = W_c(0, z) + W_{t_c}(0, z)$ is path independent. The calculation of the potential energy $v_c(0, z)$ is straightforward. However, our use of the Kolos-Roothaan wave function, in spite of its accuracy, leads to $v_c(0, z)$ being singular at the nucleus. This occurs due to the component $W_{t_c}(0, z)$ that requires a cancellation of the kinetic fields of the interacting and noninteracting systems. The underlying reason for the singularity, however, is that the wave function does not satisfy the *electron-nucleus* cusp condition exactly. In a recent paper [23], we have proved by employing the integral form of the electron-nucleus cusp condition [24], that in local effective potential energy theories and for arbitrary symmetry, the potential energy $v_{ee}(\mathbf{r})$ is finite at the nucleus. Furthermore, it is shown that this finiteness is a direct consequence of the satisfaction of the electron-nucleus cusp condition by the Schrodinger wave function. (As a consequence, for example, this potential energy is singular at each nucleus when determined either from Gaussian geminal [23] or configuration interaction [25] wave functions.) Hence, in order to obtain $v_c(0, z)$, we have employed our calculated results in regions other than near the nucleus, and smoothed the curve through each nucleus. (A comparison of our results with the work of Gritsenko *et al*[26] who in their self-consistent calculations assumed $v_{ee}(\mathbf{r})$ to be finite at the nucleus show the two curves to be indistinguishable throughout space.) The potential energy $v_c(0, z)$ is plotted in Fig.12. Observe that $v_c(0, z)$, and thus the sum of the Coulomb and Correlation-Kinetic potential energies is an order of magnitude smaller than $W_x(0, z)$, the Pauli contribution. The potential energy $v_c(0, z)$ has considerable structure, is symmetric about the origin, and is mainly positive,

indicating thereby that its principal contribution is Correlation-Kinetic. (Recall that the Coulomb field is principally negative in the right-half space (see Fig. 10) so that the Coulomb potential energy $W_c(\mathbf{r})$ is negative.) The plot of $v_c(0, z)$ translated to the right nucleus is very similar in shape and magnitude to the corresponding potential energy $v_c(\mathbf{r})$ of the Helium atom (see Fig. 4 of [2]).

To obtain a quantitative sense of the separate Coulomb and Correlation-Kinetic contributions to $v_c(0, z)$, we plot in both Figs.11 and 12 the work done $W_c(0, z)$ along the path of the nuclear bond in the force of the Coulomb field $\mathcal{E}_c(\mathbf{r})$. From $v_c(0, z)$ and $W_c(0, z)$ we obtain $W_{t_c}(0, z)$ which is also plotted in Fig. 12. The corresponding Correlation-Kinetic field $Z_{t_c}(0, z)$ is shown in Fig.13. Note that this field too is antisymmetric about the origin. Once again, there is a striking similarity between the plots of $W_c(0, z)$, $Z_{t_c}(0, z)$, and $W_{t_c}(0, z)$ when translated to the right nucleus to those of the corresponding properties of the Helium atom [2]. The Coulomb correlation part $W_c(0, z)$ is negative throughout space and vanishes by about $z = 5$ (a.u.). The Correlation-Kinetic piece $W_{t_c}(0, z)$ is throughout positive and asymptotically decays more slowly. The field $Z_{t_c}(0, z)$ is principally positive throughout space. Thus, the Correlation-Kinetic energy T_c is positive: $T = 1.1745$ (a.u.), $T_s = 1.1414$ (a.u.), $T_c = 0.0331$ (a.u.) (The corresponding value of T_c for the Helium atom is 0.0365 (a.u.)[9]). (We note that the $W_c(0, z)$ and $W_{t_c}(0, z)$ do not each separately represent a potential energy. Their sum which is $v_c(0, z)$ does.)

IV. CONCLUDING REMARKS

This paper is the first application of the Q-DFT quantal source and field perspective to a molecule, and much has been learned as explained in the previous section. The symmetry of the H_2 molecule dictates that the individual fields $\mathcal{E}_x(\mathbf{r})$, $\mathcal{E}_H(\mathbf{r})$, $\mathcal{E}_c(\mathbf{r})$, $\mathcal{Z}_{t_c}(r)$ representative of the Pauli and Coulomb correlations, and Correlation-Kinetic effects respectively, must each be antisymmetric about the center of the nuclear bond. The corresponding electron-interaction potential energy $v_{ee}(\mathbf{r})$ representative of these correlations as determined by the work done in the force of these fields is then symmetric about this point as also dictated by the symmetry of the molecule. The potential energy $v_{ee}(\mathbf{r})$ is also finite at each nucleus, as must be the case [23]. The Hartree $\mathcal{E}_H(\mathbf{r})$ and Pauli $\mathcal{E}_x(\mathbf{r})$ fields are the largest in magnitude and opposite in sign, the former being positive and twice as large as the latter. As such the principal contributions to

the electron-interaction energy E_{ee} and potential energy $v_{ee}(\mathbf{r})$ are due to the Hartree and the Pauli correlation terms. The Coulomb $\mathcal{E}_c(\mathbf{r})$ and Correlation-Kinetic $\mathcal{Z}_{t_c}(r)$ fields tend to cancel each other, so that the contribution of their sum to the potential energy $v_{ee}(\mathbf{r})$ is an order of magnitude smaller. However, as the potential energy component $v_c(\mathbf{r})$ representing the sum of these correlations is principally positive (see Fig. 12), it is evident that the Correlation-Kinetic effects are more significant. They are also more significant asymptotically, where the Coulomb correlation contributions to the potential energy vanish. Thus, Correlation-Kinetic effects play an important role in local effective potential energy theories of the H_2 molecule. We further note that in the construction of approximate KS-DFT ‘exchange-correlation’ and correlation energy functionals $E_{xc}^{KS}[\mathbf{r}]$ and $E_c^{KS}[\mathbf{r}]$ for molecules, Correlation-Kinetic effects must be incorporated if an accurate S system representation of molecules is to be obtained.

On the basis of the Q-DFT results determined from the H_2 molecule, it is evident that the qualitative features of the quantal sources, fields, and potential energies for other diatomic molecules will be similar. However, the fields and hence the potential energies of these diatomics will have more structure as a consequence of the additional molecular subshells. We expect this added structure to be similar to that observed in atoms as the number of shells is increased. Finally, we note that the accuracy of approximation methods within Q-DFT [27] and KS-DFT can be tested by comparison with these essentially exact results.

We conclude by reiterating the striking similarity between the Q-DFT properties of the Hydrogen molecule and the Helium atom for electron positions in the positive half space. It is interesting that in spite of the presence of a second nucleus, and therefore of a different symmetry, the quantal sources and fields representative of the various electron correlations in the Hydrogen molecule are so similar to those of the Helium atom. This speaks to the commonality of properties of these distinct quantum systems as exhibited within the framework of Q-DFT.

Acknowledgments

We thank Prof. E. J. Baerends and Dr. Myrta Grüning for sending us the results of Ref. [26]. This work was supported in part by the Research Foundation of the City University of New York.

TABLE I: Variational parameters in the normalized 51-parameter correlated wave function for the ground state of H_2 [11].

No. of terms					50
$\delta =$					0.995
ξ_1	η_1	ξ_2	η_2	r_{12}	Coefficients
0	0	0	0	0	2.065908
0	0	0	2	0	1.282032
0	0	1	0	0	0.144619
0	1	0	1	0	-0.430253
0	0	0	0	1	0.787198
1	1	0	1	0	-0.235454
1	0	0	2	0	0.148273
0	0	2	0	0	0.109859
0	0	0	0	2	-0.212159
1	0	1	0	0	-0.081387
0	2	0	2	0	0.182892
0	0	0	2	1	0.198555
0	0	1	0	1	0.324658
1	1	1	1	0	-0.010794
0	0	1	0	2	0.077830
1	0	2	0	0	-0.055114
0	1	0	1	1	0.130714
0	1	0	1	2	-0.050854
1	0	2	0	1	0.014963
0	0	2	0	1	-0.132980
1	1	1	1	2	0.000362
0	0	2	0	2	0.006992
1	0	0	2	1	-0.050940
1	1	1	1	1	0.018027
1	0	1	0	1	0.017554
0	0	0	2	2	-0.014601
1	0	1	0	2	-0.015172
1	0	0	2	2	0.012656
1	2	3	0	0	-0.000202
2	0	3	0	0	-0.000856
0	0	1	2	0	-0.009469
0	0	3	0	0	0.036963
1	0	1	2	0	-0.022325
0	1	2	1	0	0.053233
1	0	3	0	0	0.004690
1	2	1	2	0	0.004707
1	1	2	1	0	-0.017531
0	2	3	0	0	0.017270
3	0	3	0	0	0.000082
2	1	2	1	0	0.000031
0	0	1	2	1	0.094436
0	0	3	0	1	0.001789
0	0	3	0	2	-0.000394
0	0	1	2	2	-0.004475
2	0	3	0	1	-0.000121
1	0	1	2	1	-0.014893
2	0	3	0	2	0.000011
1	0	1	2	2	0.001016
0	2	3	0	1	-0.003443
0	2	3	0	2	0.000225

APPENDIX: Wave function parameters

The values of the parameter δ and the coefficients c_{mnjkp} for the wave function of Eq.(21) are listed in the table I.

[1] V. Sahni, Phys. Rev A **55**, 1846(1997).

[2] V. Sahni, Top. Curr. Chem. **182**, 1(1996).

- [3] Z. Qian and V. Sahni, Phys. Rev. A **57**, 2527(1998).
- [4] Z. Qian and V. Sahni, Phys. Rev. B **62**, 16364(2000).
- [5] V. Sahni, L. Massa, R. Singh and M. Slamet, Phys. Rev. Lett. **87** 113002(2001).
- [6] M. Slamet and V. Sahni, Int. J. Quantum Chem. **85** 436(2001).
- [7] V. Sahni and X.-Y. Pan, Phys. Rev. Lett. **90**, 123001 (2003).
- [8] M. Slamet, R. Singh, L. Massa, and V. Sahni, (submitted to Phys. Rev. A).
- [9] M. Slamet and V. Sahni, Phys. Rev. A **51**, 2815 (1995).
- [10] *Atoms and atomic ions*: V. Sahni in *Structure and Dynamics of Atoms and Molecules: Conceptual Trends*, edited by J. L. Calais and E. S. Kryachko, (Kluwer Academic Publishers, 1995); V. Sahni, Y. Li, and M. K. Harbola, Phys. Rev. A **45**, 1434 (1992). *Atomic excited states*: R. Singh and B. M. Deb, Phys. Rep. **311**, 47 (1999). *Positron binding*: R. R. Zope, Phys. Rev. A **60**, 218 (1999). *Metallic surfaces*: V. Sahni and A. Solomatin, Adv. Quantum Chem. **33**, 241 (1999). *Metallic clusters*: M. K. Harbola, J. Chem. Phys. **97**, 2578 (1992).
- [11] W. Kolos and C. C. J. Roothaan, Rev. Mod. Phys. **32**, 219 (1960).
- [12] W. Kohn and L. J. Sham, Phys. Rev. **140**, A1133 (1965).
- [13] J. P. Perdew, R. G. Parr, M. Levy, and J. L. Balduz, Phys. Rev. Lett. **49**, 1691(1982); M. Levy, J. P. Perdew, and V. Sahni, Phys. Rev. A **30**, 2745 (1984); C.-O. Almbladh and U. von Barth, Phys. Rev. B **31**, 3231 (1985).
- [14] A. Gorling, Phys. Rev. A **46**, 3753 (1992).
- [15] Y. Wang and R. G. Parr, Phys. Rev. A **47**, R1591 (1993).
- [16] R. Van Leeuwen and E. J. Baerends, Phys. Rev. A **49**, 2421 (1994).
- [17] Q. Zhao, R. C. Morrison, and R. G. Parr, Phys. Rev. A **50**, 2138 (1994).
- [18] H. Wind, J. Chem. Phys. **42**, 2371 (1965); D. R. Bates, K. Ledsham, and A. L. Stewart, Phil. Trans. Roy. Soc. A **246**, 215 (1953).
- [19] M. Taut, Phys. Rev. A **48**, 3561 (1993).
- [20] T. Kato, Commun. Pure. Appl. Math. **10**, 151 (1957); E. Steiner, J. Chem. Phys. **39**, 2365 (1963).
- [21] W. Kolos and C. C. J. Roothaan, Rev. Mod. Phys. **32**, 205 (1960).
- [22] E. J. Baerends, Phys. Rev. Lett. **87**, 133004 (2001); E. J. Baerends and O. V. Gritsenko, J. Phys. Chem. A **101**, 5383 (1997); R. van Leeuwen, O. V. Gritsenko, and E. J. Baerends, Top. Curr. Chem. **180**, 107 (1996).
- [23] X.-Y. Pan and V. Sahni, Phys. Rev. A **67**, 012501 (2003).
- [24] W. A. Bingel, Z. Naturforsch. A **18a**, 1249 (1963); Theor. Chim. Acta (Berl) **8**, 54 (1967); R. T. Pack and W. Byers Brown, J. Chem. Phys. **45**, 556 (1966).
- [25] M. E. Mura, P. J. Knowles, and C. A. Reynolds, J. Chem. Phys. **106**, 9659 (1997).
- [26] O. V. Gritsenko, R. van Leeuwen, and E. J. Baerends, Phys. Rev. A **52**, 1870 (1995).
- [27] R. Singh, L. Massa, and V. Sahni, Phys. Rev. A **60**, 4135(1999).

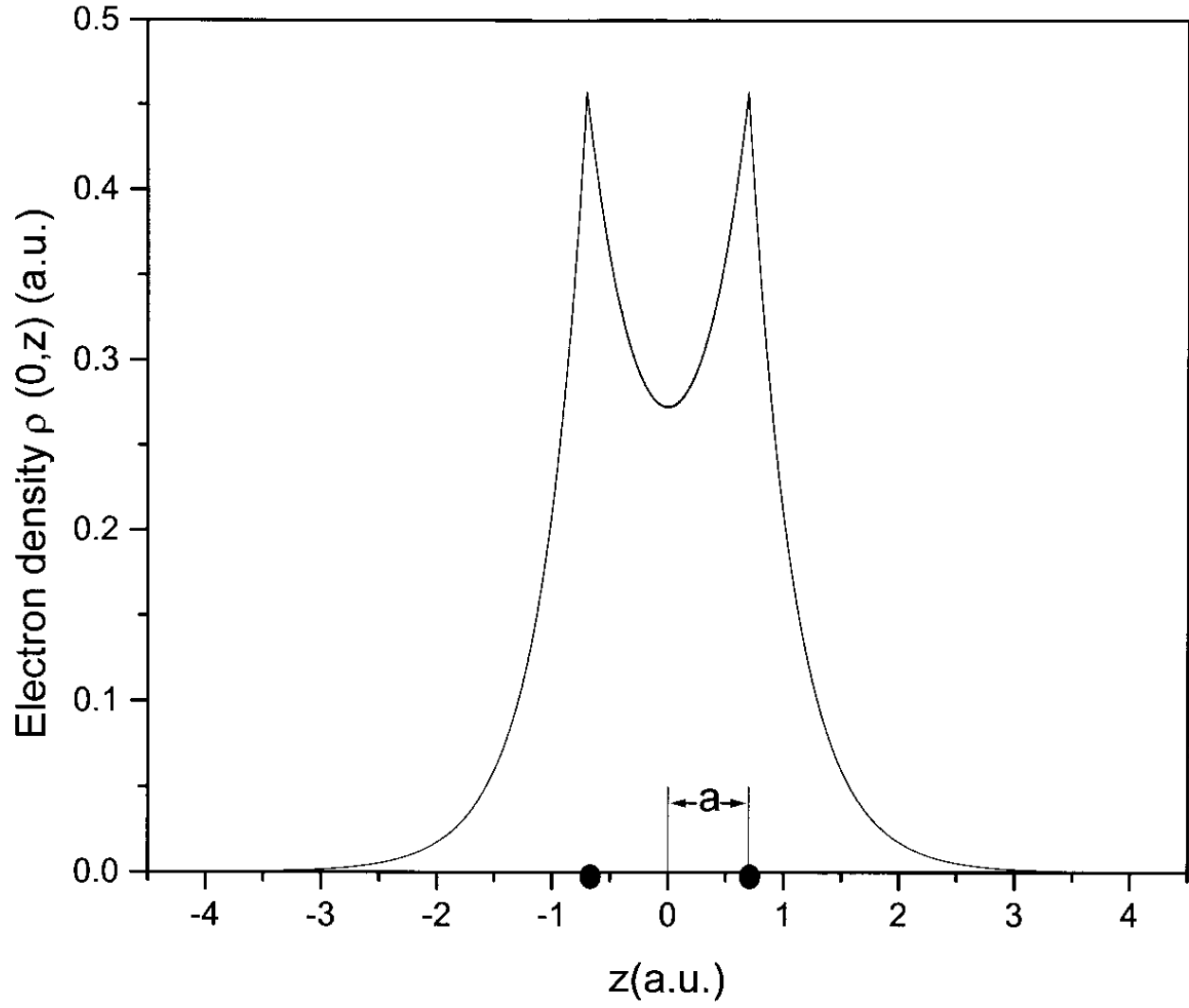


FIG. 1: The electron density $\rho(0, z)$ of the hydrogen molecule along the nuclear bond axis in atomic units (a.u.). The nuclei are on the axis at $a = 0.7005$ (a.u.) indicated by the two dots.

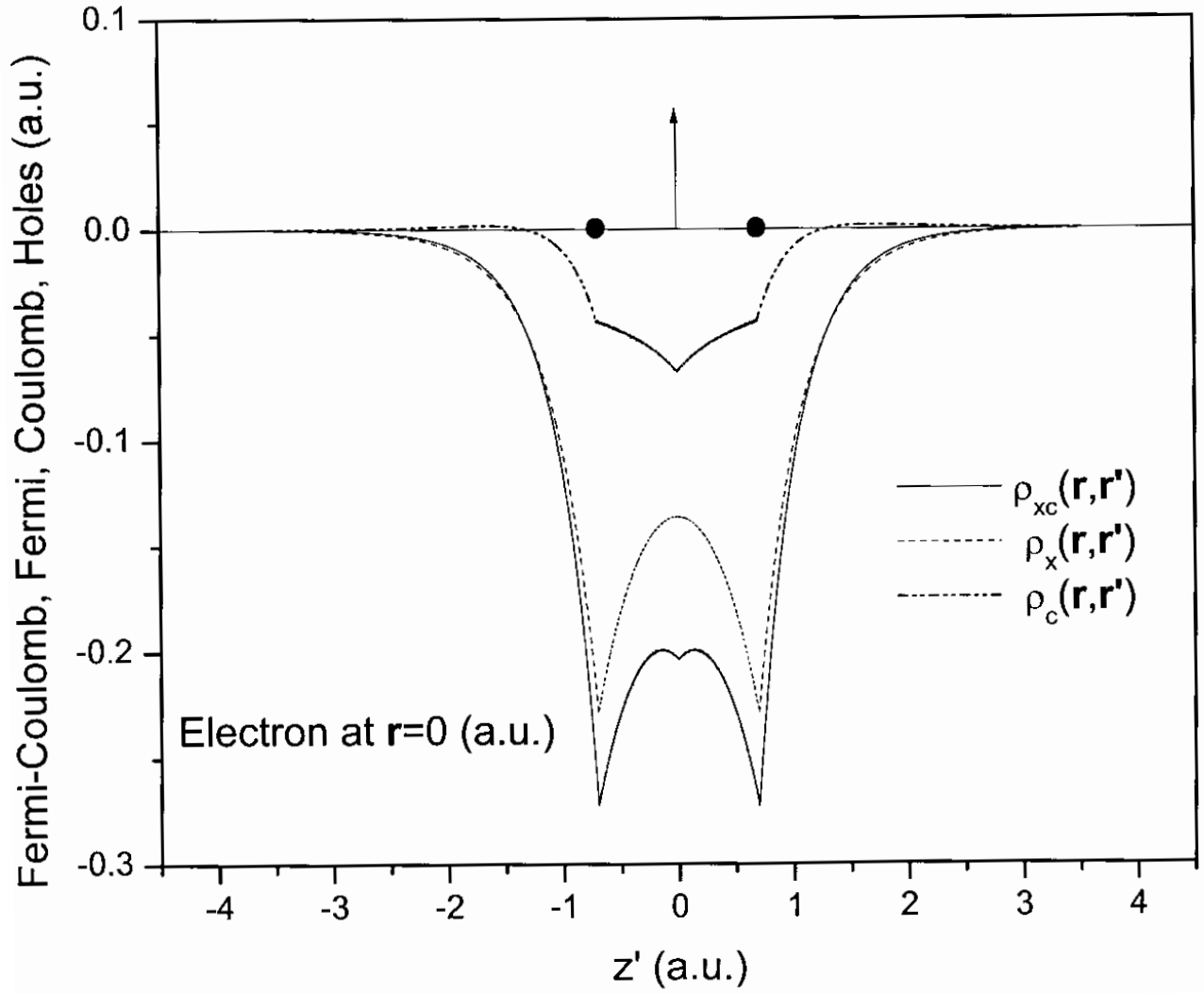


FIG. 2: Cross-sections of the Fermi-Coulomb $\rho_{xc}(\mathbf{r}, \mathbf{r}')$, Fermi $\rho_x(\mathbf{r}, \mathbf{r}')$, and Coulomb $\rho_c(\mathbf{r}, \mathbf{r}')$ holes along the nuclear bond axis for an electron at the center $\mathbf{r} = (0, 0)$ of the bond. The electron position is indicated by the arrow.

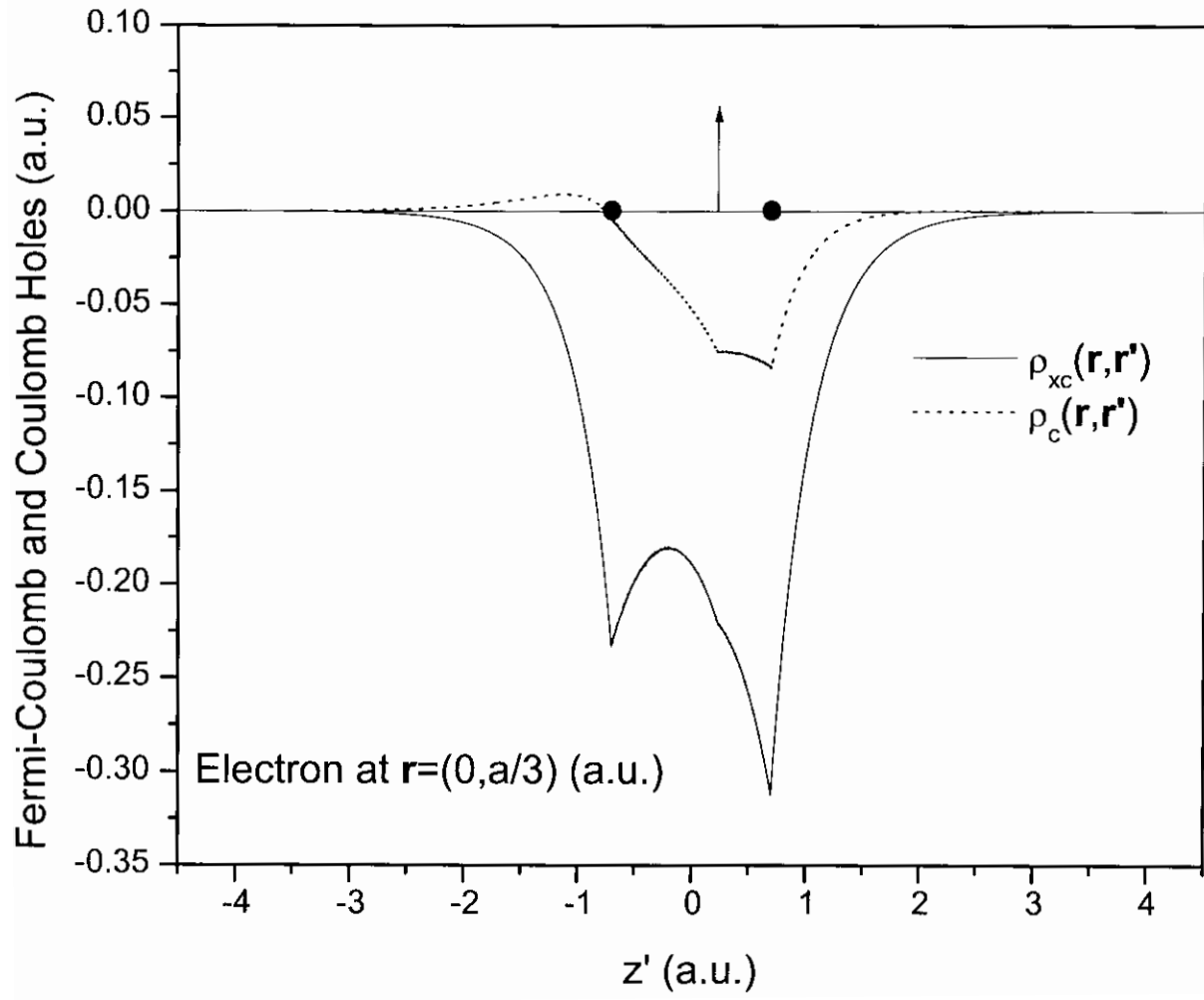


FIG. 3: Cross-sections of the Fermi-Coulomb $\rho_{xc}(\mathbf{r}\mathbf{r}')$ and Coulomb $\rho_c(\mathbf{r}\mathbf{r}')$ holes along the nuclear bond axis for an electron at the center $\mathbf{r} = (0, a/3)$ of the bond with the electron position indicated by the arrow.

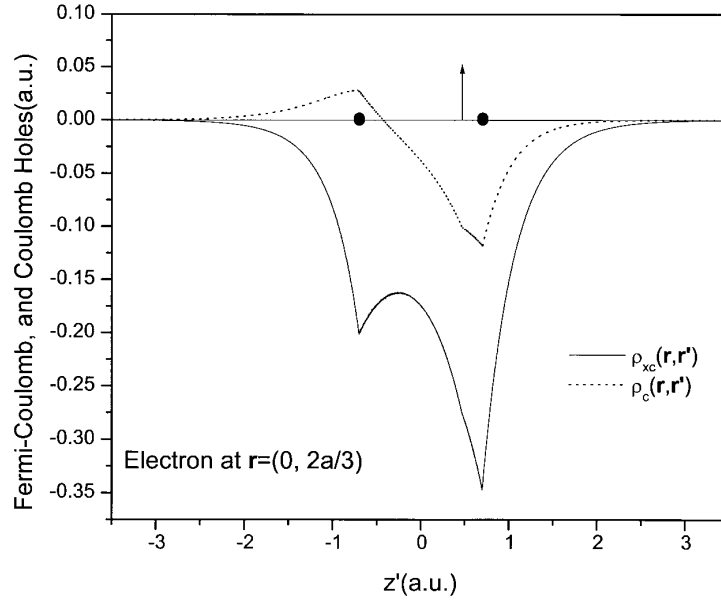


FIG. 4: The same as in Fig.3, but with the electron at $\mathbf{r} = (0, 2a/3)$.

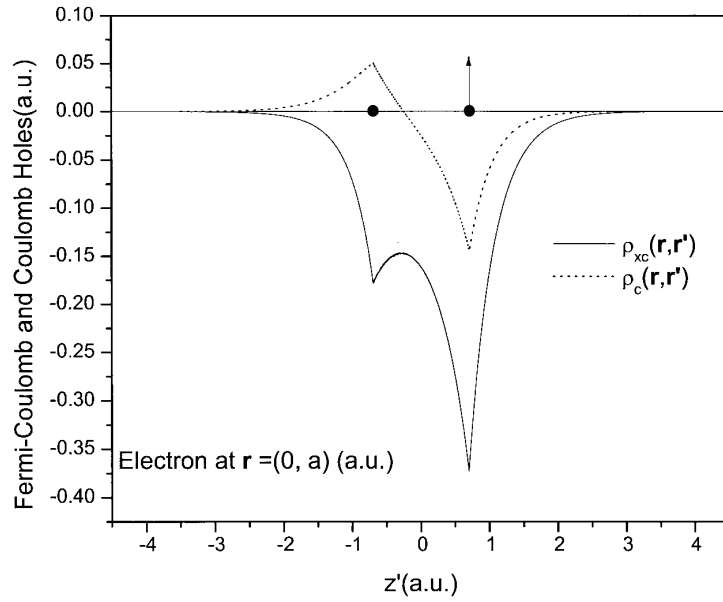


FIG. 5: The same as in Fig.3, but with the electron at $\mathbf{r} = (0, a)$.

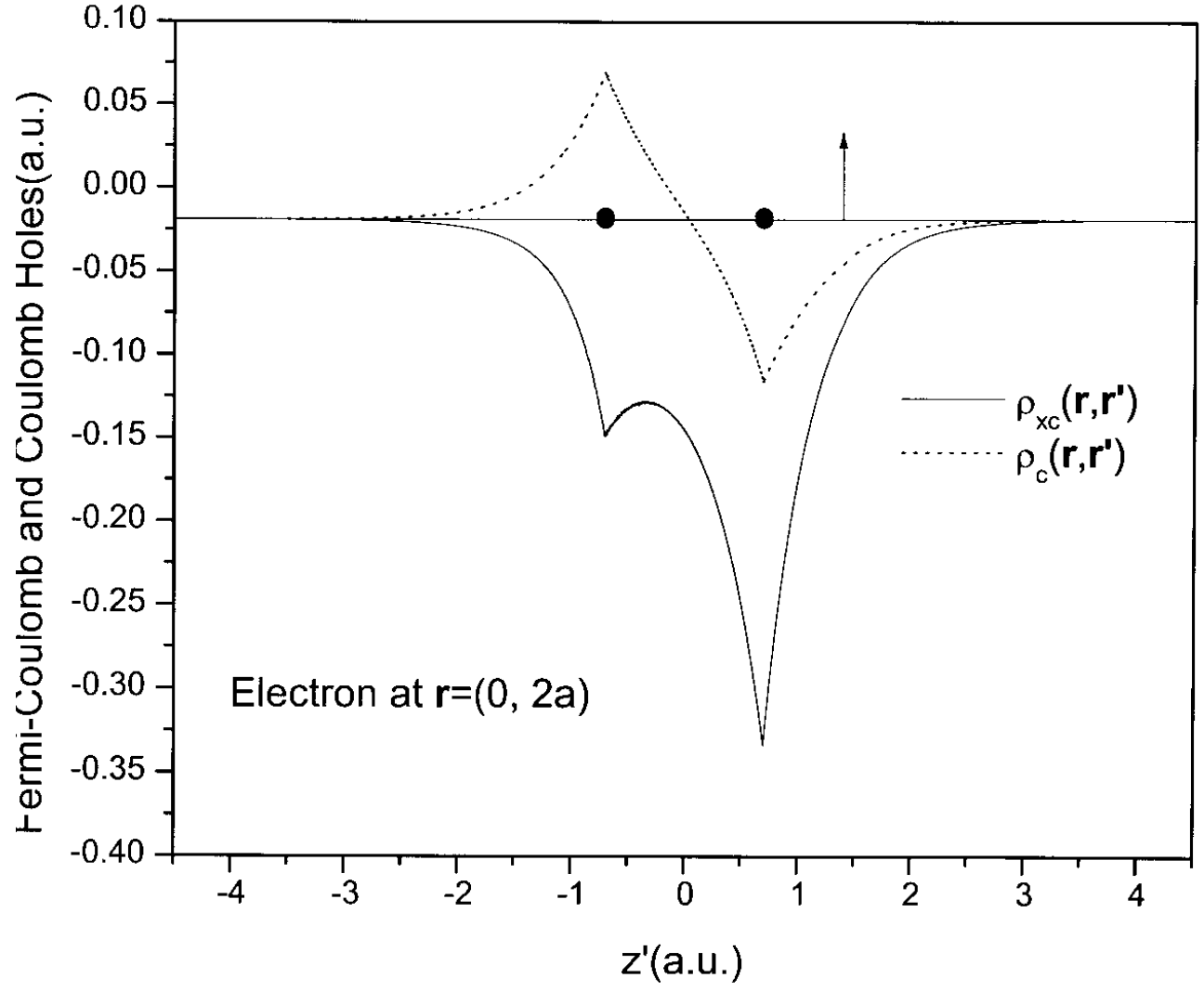


FIG. 6: The same as in Fig.3, but with the electron at $\mathbf{r} = (0, 2a)$.

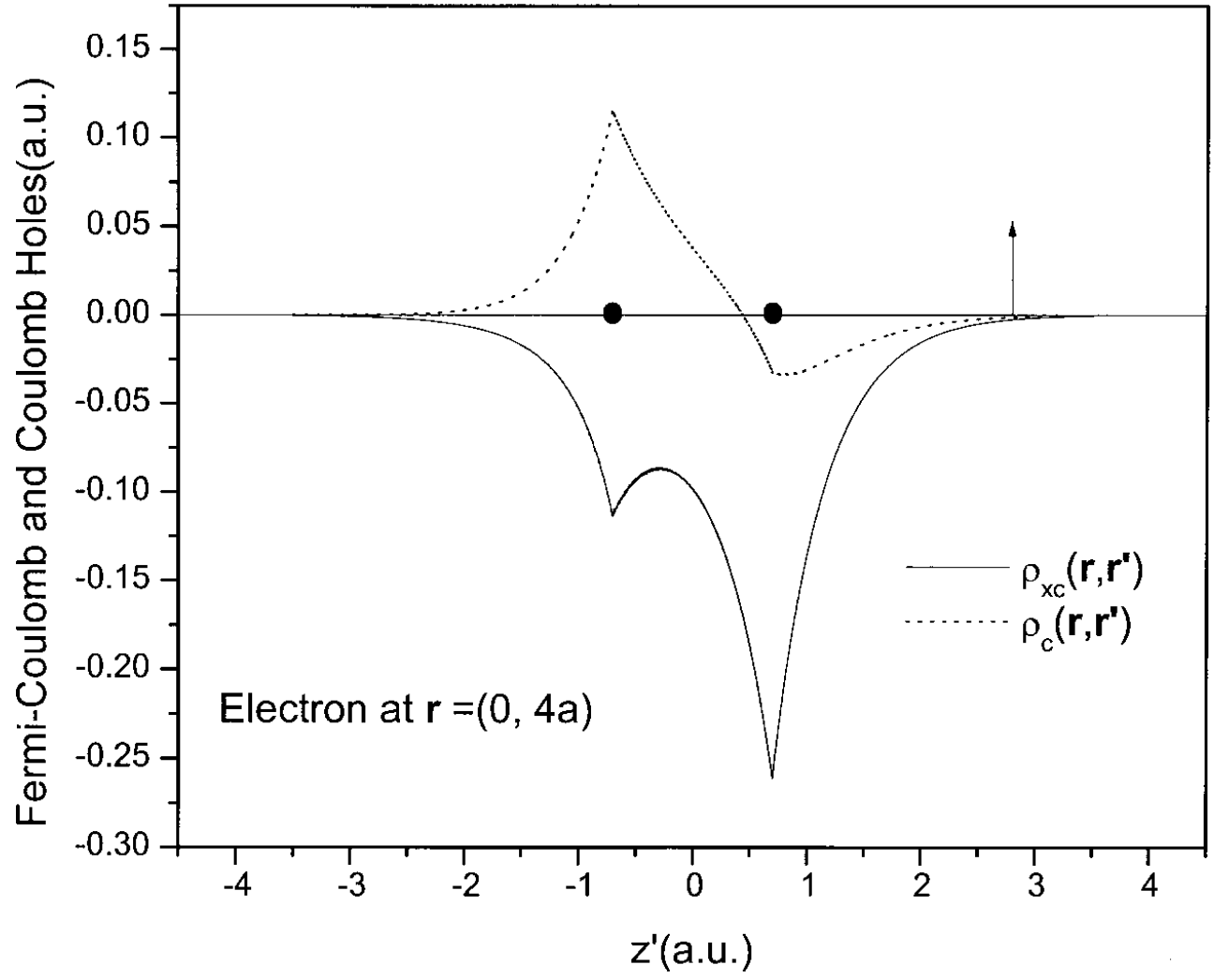


FIG. 7: The same as in Fig.3, but with the electron at $\mathbf{r} = (0, 4a)$.

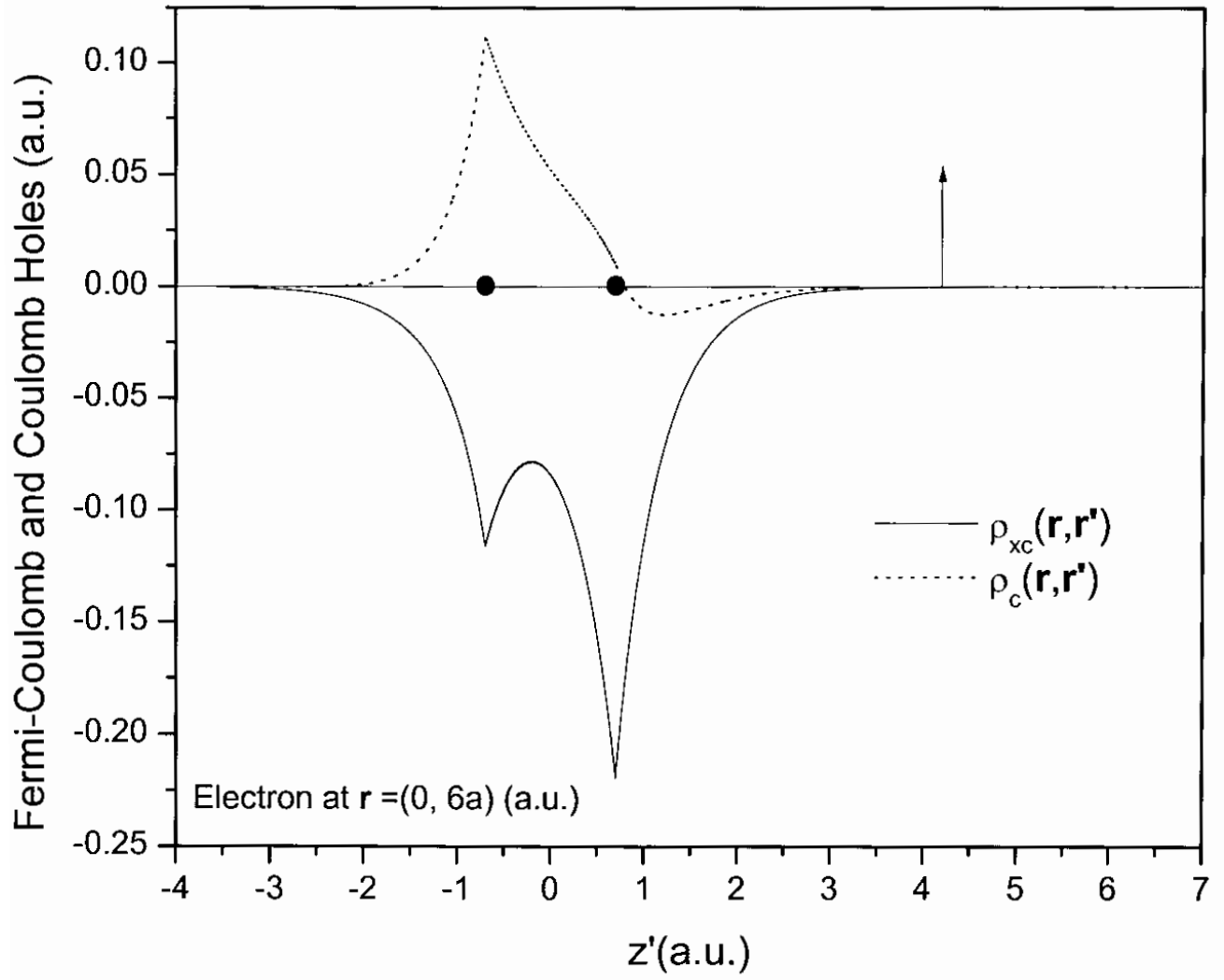


FIG. 8: The same as in Fig.3, but with the electron at $\mathbf{r} = (0, 6a)$.

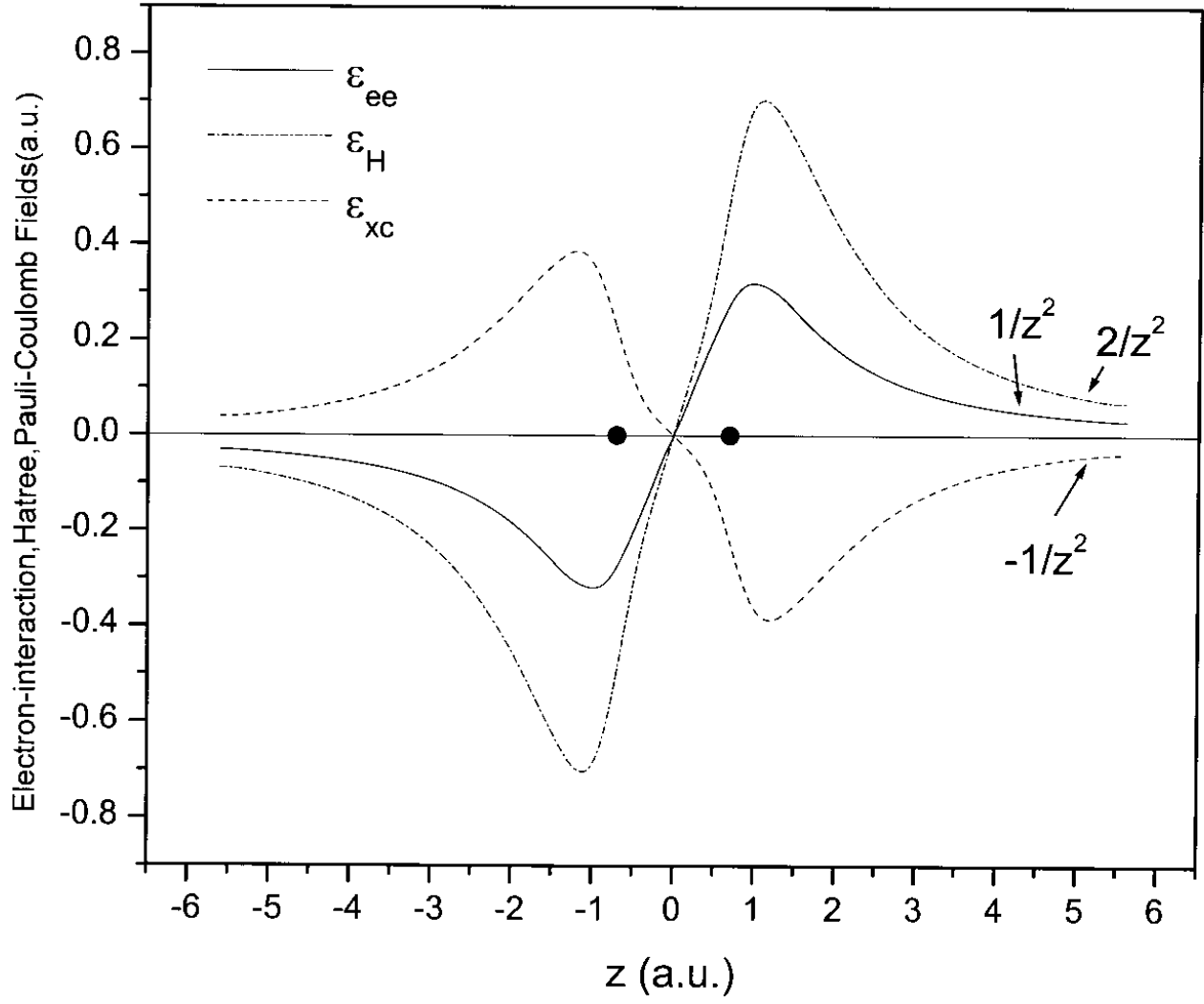


FIG. 9: The electron-interaction $\mathcal{E}_{ee}(0, z)$ field, and its Hartree $\mathcal{E}_H(0, z)$ and Pauli-Coulomb $\mathcal{E}_{xc}(0, z)$ components along the nuclear bond axis.

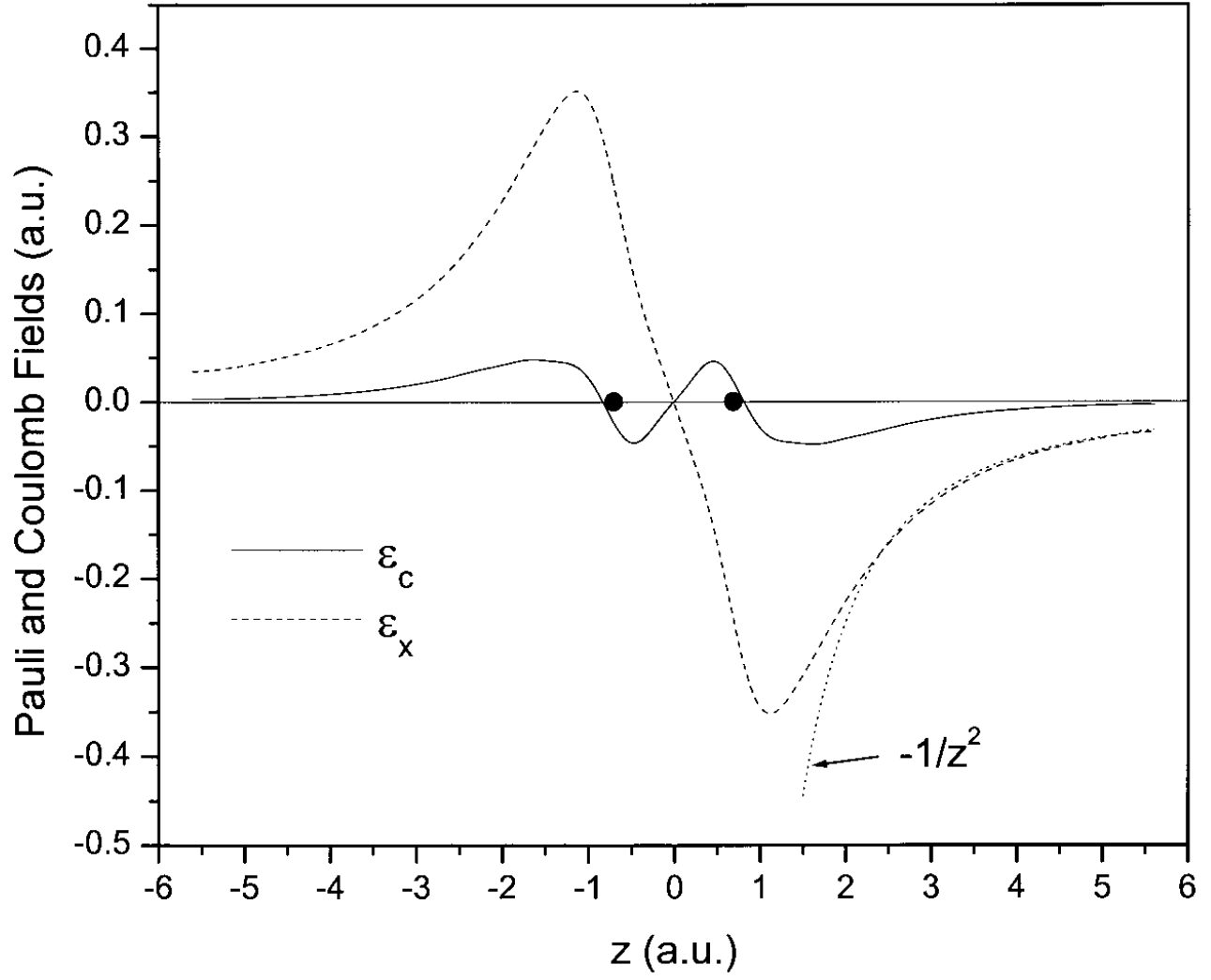


FIG. 10: The Pauli $\epsilon_x(0, z)$ and Coulomb $\epsilon_c(0, z)$ fields along the nuclear bond axis. The function $-1/z^2$ is also plotted.

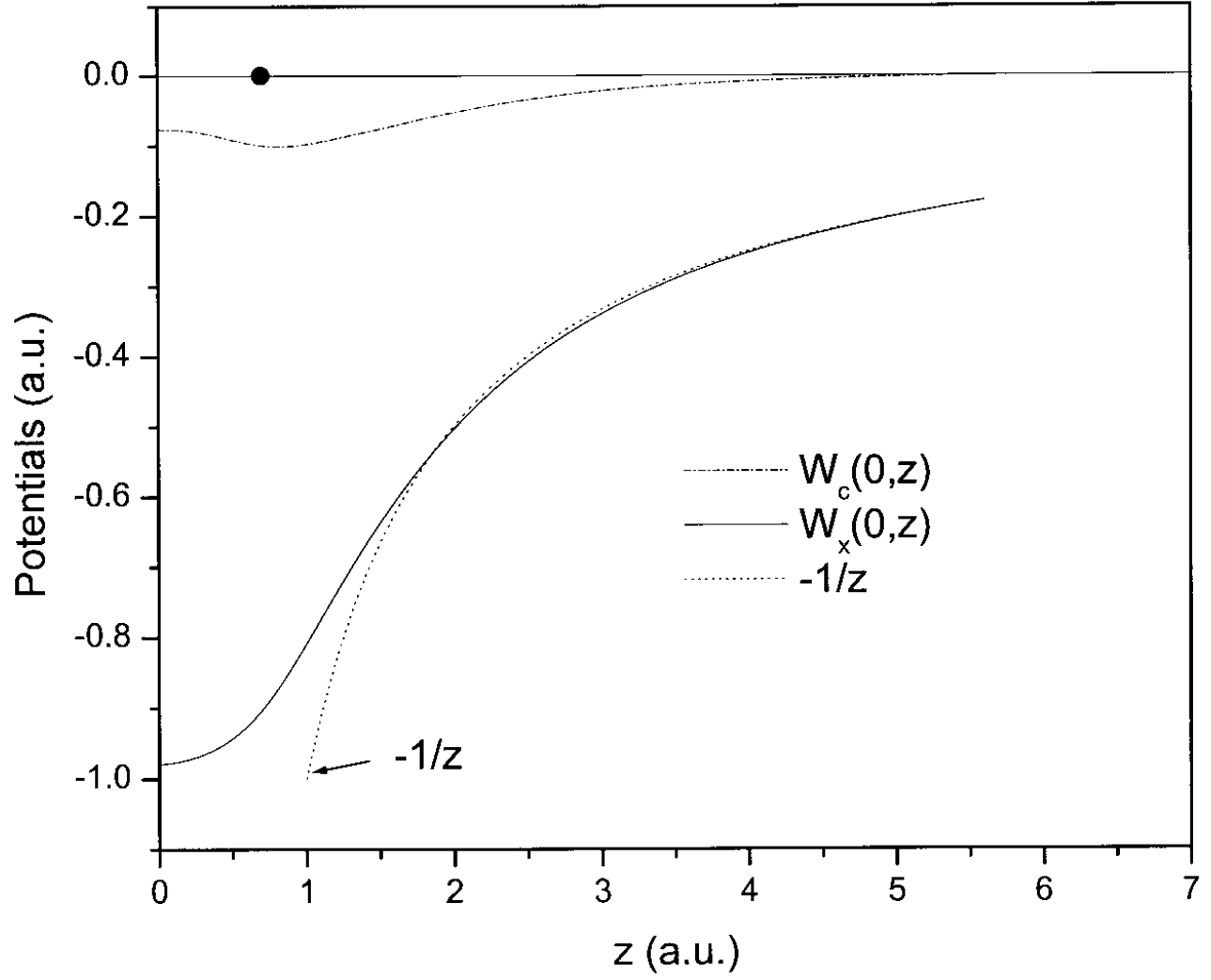


FIG. 11: The Pauli potential energy $W_x(0, z)$ along the nuclear bond axis. The work done $W_c(0, z)$ in this direction in the force of the Coulomb field $\mathcal{E}_c(0, z)$, and the function $-1/z$, are also plotted.

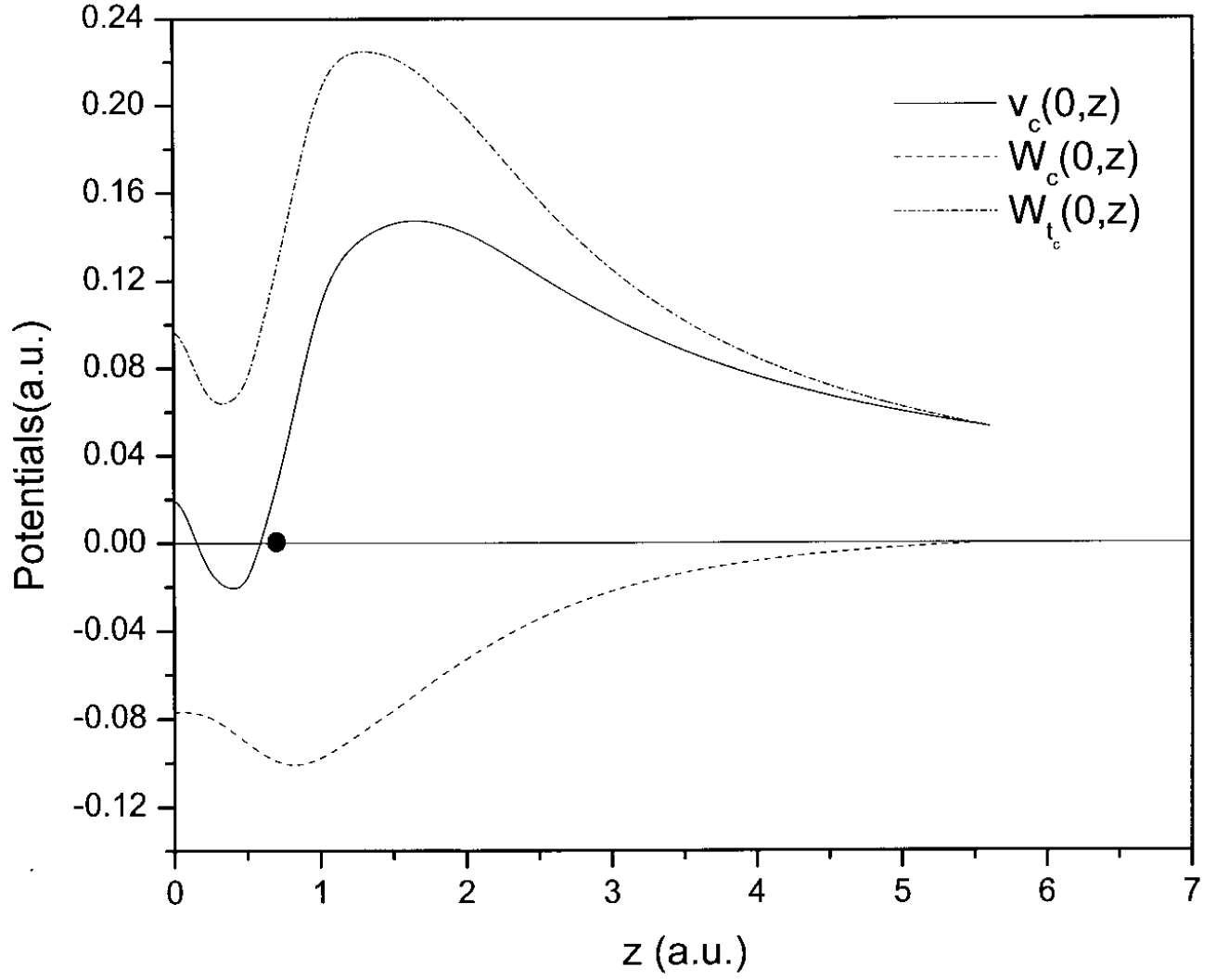


FIG. 12: The potential energy $v_c(0, z)$, the sum of the Coulomb and Correlation-Kinetic potential energies, along the nuclear bond axis. The work done $W_c(0, z)$ of Fig. 11, and the work done $W_{t_c}(0, z)$ in the force of the Correlation-Kinetic field $\mathcal{Z}_{t_c}(0, z)$ of Fig.13, are also plotted.

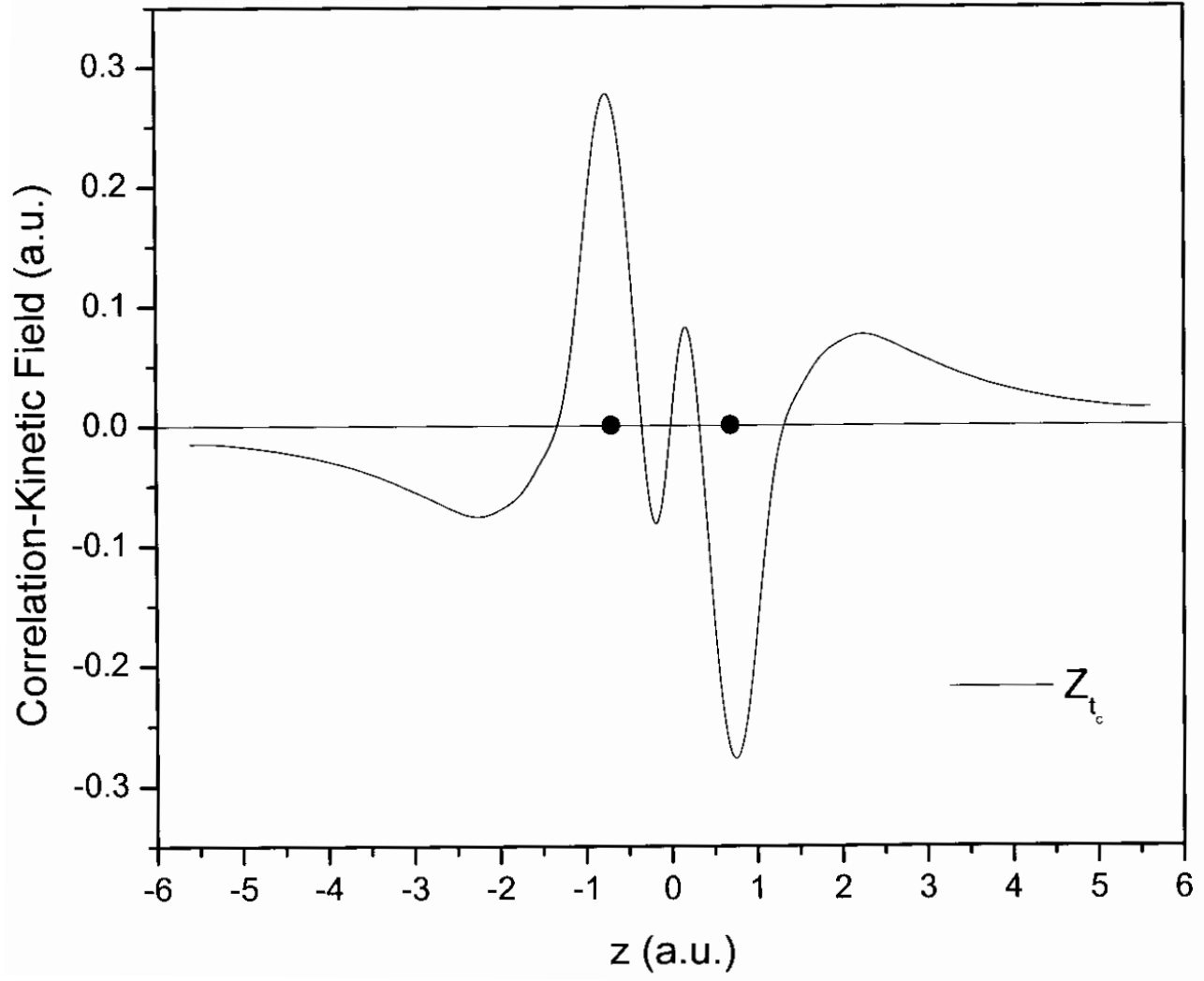


FIG. 13: The Correlation-Kinetic field $Z_{t_c}(0, z)$ along the nuclear bond axis.